Journal of Inorganic and General Chemistry
ZAAC
Zeitschrift für anorganische und allgemeine Chemie
www.zaac.wiley-vch.de
RESEARCH ARTICLE
DOI: 10.1002/zaac.202300249

Special Collection

Isolation of an Osmium(III) Hydrido Complex

Niyaz Alizadeh,[a] Josh Abbenseth,[b] Sarah Bete,[a] Markus Finger,[a] Matthias Otte,[a] Christian Würtele,[c] and Sven Schneider*[a]

Dedicated to Professor Rhett Kempe on the occasion of his 60th birthday.

Synthesis and characterization of $[OsH(PNP)(bipy)]^+$ (PNP = $N(CHCHP^tBu_2)_2$) are reported, as the second osmium(III) hydrido complex next to $[OsH(en)_2(py)]^{2+}$. While the osmium(II) precursor, [OsH(PNP)(bipy)], exhibits two reversible oxidations in the cyclic voltammogram, the product from 2-electron oxidation could not be isolated due to rapid decay. Thermochemical examinations attribute the stability of the osmium(III) hydride to both thermodynamic and kinetic reasons. In contrast, the high estimated acidity of $[OsH(PNP)(bipy)]^{2+}$ presumably leads to rapid decay.

Introduction

Transition metal hydrido complexes are key species in catalysis, such as de-/hydrogenation reactions.[1,2] The current renaissance of molecular electrocatalysis revived an interest in understanding and controlling the stability of organometallic radical species, such as open-shell hydrides.[3] Norton and co-workers pointed out that transition metal hydrido radical cations often suffer from lower chemical stability.[4] Various decay pathways are conceivable even for the simplest case, i.e., monohydrides, as showcased by seminal studies from Tilset and Parker:[5] On one hand, oxidation reduces the homolytic M–H bond strength. Hydrides become thermodynamically unstable towards H_2 evolution, if the bond dissociation free energy ($BDFE_{M-H}$) drops below that of H_2 ($0.5 \cdot BDFE_{H2}{}^{THF} = 52.0$ kcal mol^{-1}).[6] On the other hand, oxidation typically increases the M–H acidity by more than 20 pK_a units,[7] potentially rendering the oxidized state susceptible to metal deprotonation. However, more data is needed to relate the thermodynamic stability and kinetic inertness of hydrido radical cations to chemical structure and reaction conditions, such as the solvent.

We here report a case study about the thermochemical stability and kinetic inertness of a transition metal hydrido radical cation. We chose osmium, as Taube's $[OsH(en)_2(py)]^{2+}$, surprisingly is the only isolable osmium(III) hydride reported in the literature.[8] Furthermore, two dichotomous ligands were employed to evaluate the potential impact of ligand redox non-innocence on the Os–H bond strength: an anionic, unsaturated PNP pincer ligand,[9] which can stabilize high-valent metal radical complexes by spin delocalization,[10] as well as 2,2′-bipyridine (bipy) as archetypal redox-active ligand in low-valent states.[11]

[a] N. Alizadeh, Dr. S. Bete, Dr. M. Finger, M. Otte, Prof. Dr. S. Schneider
Institut für Anorganische Chemie
Georg-August-Universität
Tammannstraße 4, 37077 Göttingen (Germany)
E-mail: sven.schneider@chemie.uni-goettingen.de
[b] Dr. J. Abbenseth
Institut für Chemie
Humboldt-Universität zu Berlin
Brook-Taylor-Straße 2, 12489 Berlin (Germany)
[c] Dr. C. Würtele
Institut für Anorganische und Analytische Chemie
Justus-Liebig-Universität Gießen
Heinrich-Buff-Ring 14, 35392 Gießen (Germany)

Supporting information for this article is available on the WWW under https://doi.org/10.1002/zaac.202300249

This article is part of a Special Collection dedicated to Professor Rhett Kempe on the occasion of his 60th birthday. Please see our homepage for more articles in the collection.

Results and Discussion

Syntheses of five-coordinate complexes. Our group recently reported the synthesis of osmium(III) pincer complex $[OsCl_2(PNP)]$ (**1**; PNP = $N(CHCHP^tBu_2)_2$). Reduction of **1** gave access to an unprecedented, square-planar osmium(II) complex with a spin triplet ground state, $[Os^{II}Cl(PNP)]$, which is an excellent precursor for the introduction of additional ligands.[12]

In situ reduction of **1** and subsequent addition of bipy gave $[Os^{II}Cl(PNP)(bipy)]$ (**2**) in 74% isolated yield (Scheme 1). Structural analysis of the diamagnetic d^6 complex confirmed distorted octahedral metal coordination and typical bond lengths for low-spin osmium(II) (Figure 1). Starting from parent **1**, the five-coordinate {Os(PNP)(bipy}-platform was accessed by reduction in the presence of bipy and subsequent chloride removal with $NaBPh_4$ or $NaBAr^F{}_4$ ($BAr^F{}_4{}^- = B(C_6H_3\text{-}3,5\text{-}(CF_3)_2)_4{}^-$). The cationic complex $[Os^{II}(PNP)(bipy)]^+$ (**3**$^+$; Scheme 1) was isolated as tetraarylborate salts in moderate yields up to around 50%. Single-crystal X-ray diffraction of **3**^{BPh4} confirmed distorted square-pyramidal coordination ($\tau = 0.30$; Figure 1).[13] However, the NMR data at room temperature revealed C_{2v} symmetry in

Journal of Inorganic and General Chemistry
ZAAC
Zeitschrift für anorganische und allgemeine Chemie

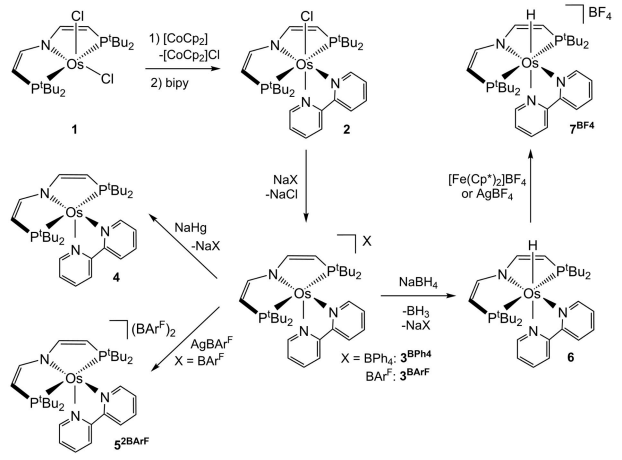

Scheme 1. Syntheses of osmium complexes **2**–**7**^{BF4}.

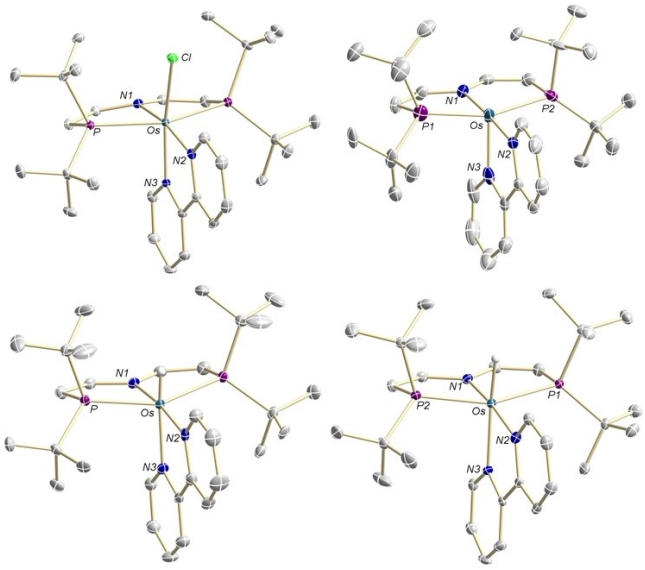

Figure 1. Molecular structures of **2** (top left), **3**^{BPh4} (top right), **6** (bottom left), and **7**^{BF4} (bottom right) from single-crystal X-ray diffraction (thermal ellipsoids at the 50 % probability level); hydrogen atoms except the hydride ligands, solvent molecules and counter-anions are omitted for clarity. Selected bond lengths in [Å] and angles [°]: **2**: Os–Cl 2.4557(6), Os–N1 2.120(2), Os–N2 2.060(2), Os–N3 2.031(2), Os–P 2.4352(5), P–Os–P$^{\#}$ 156.05(2), N1–Os–Cl 107.00(6), N2–Os–Cl 85.85(6), N3–Os–Cl 165.01(6); **3**^{BPh4}: Os–N1 2.015(4), Os–N2 2.036(2), Os–N3 2.039(3), Os–P1 2.3676(7), Os–P2 2.3852(7), P1–Os–P2 160.29(2), N1–Os–N2 176.59(14), N1–Os–N3 98.98(14); **6**: Os–N1 2.103(5), Os–N2 2.021(5), N3–Os 2.096(5), Os–P 2.3621(11), P–Os–P$^{\#}$ 152.17(5), N1–Os–N2 170.1(2), N1–Os–N3 92.14(18); **7**^{BF4}: Os–H: 1.53(4), Os–N1 2.012(4), Os–N2 2.085(3), Os–N3 2.141(3), Os–P1 2.3774(11), Os–P2 2.3809(11), P1–Os–P2 157.19(4), N1–Os–N2 171.14(14), N1–Os–N3 94.89(14).

solution, due to fluxional bipy coordination on the NMR time scale.

Electrochemical characterization of **3**^{BPh4} by cyclic voltammetry (CV) featured two reversible reductions at $E^0 = -1.83$ and -2.55 V vs. Fc^+/Fc, respectively (Figure 2).[14] While the reduced species could not be cleanly isolated, *in situ* reduction of **3**$^+$ with Na/Hg ($E \approx -2.4$ V)[15] allowed for EPR spectroscopic characterization of the first reduction product. The X-band EPR spectrum in frozen solution (Figure 3) features a rhombic signal ($S = 1/2$) with relatively small g-anisotropy ($g = 2.02, 1.97, 1.90$) for a heavy metal complex. Furthermore, the resolved hyperfine interaction (HFI) was simulated with two ^{14}N and two ^{1}H nuclei.[16] Thus, the EPR data as well as the range of the reduction potential support predominantly bipy-centered reduction, tantamount to formation of [Os^{II}(PNP)(bipy$^{-\bullet}$)] (**4**).[17] This notion is fully supported by DFT computations, which nicely reproduced the experimental EPR spectrum and localized 92 % of the spin density at the bipy ligand (Figure 3).

Besides the reductive events, the CV of **3**^{BPh4} also shows a reversible oxidation wave at $E^0 = 0.06$ V (Figure 2) with relatively large peak-to-peak separation (> 200 mV) that increases with scan rate, indicating slow heterogeneous electron transfer. The thermally sensitive oxidation product, [Os(bipy)(PNP)](BAr^F)$_2$ (**5**^{2BArF4}), was synthesized upon chemical oxidation of **3**^{BArF4} with AgBAr$^F_4$ in THF at −80 °C (Scheme 1). Spectroscopic characterization of **5**^{2BArF4} was carried out by EPR spectroscopy. The signal could be fitted for a spin doublet ground state with distinct rhombicity ($g = 2.35, 2.00, 1.78$; Figure 3), as expected for a d^5 ion in low symmetry ligand field.[18] The spectrum was nicely reproduced by DFT ($g_{DFT} = 2.29, 2.00, 1.86$) for the computed square-pyramidal coordination geometry (Figure 3). Interestingly, the computations revealed predominant $\pi^*(p_N/d_{Os})$-character of the SOMO with significant spin delocalization to the PNP ligand (≈ 70 %, Figure 3), underlining the capability of the pincer ligand to stabilize radical complexes by π-redox non-innocence.

Syntheses of octahedral hydrido complexes. The introduction of a hydrido ligand is best carried out from the five-coordinate complex **3**^{BPh4}. Reaction with excess $NaBH_4$ allowed for isolating [Os^{II}H(PNP)(bipy)] (**6**) in 58 % yield. The presence of the hydride was confirmed by ^{1}H NMR spectroscopy ($\delta_H = -11.0$ ppm) and the band in the infrared spectrum at $\tilde{\nu}_{Os-H} = 2100\ cm^{-1}$ (DFT: 2096 cm^{-1}). The frequency of the Os–H stretching mode is at the upper end of the typical range found for octahedral d^6 hydrido complexes,[19] and specifically for Os^{II} hydrides,[20] suggesting strong Os–H bonding. The presence of the hydride is further reflected in the molecular structure

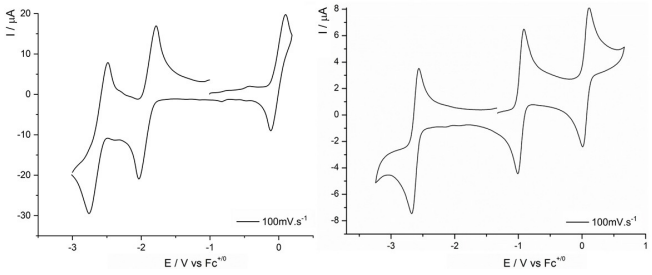

Figure 2. Cyclic voltammograms of **3**^{BPh4} (left) and **6** (right) in THF at room temperature (c = 1.0 mM, 0.1 M NBu_4PF_6, $v = 100$ mV s^{-1}).

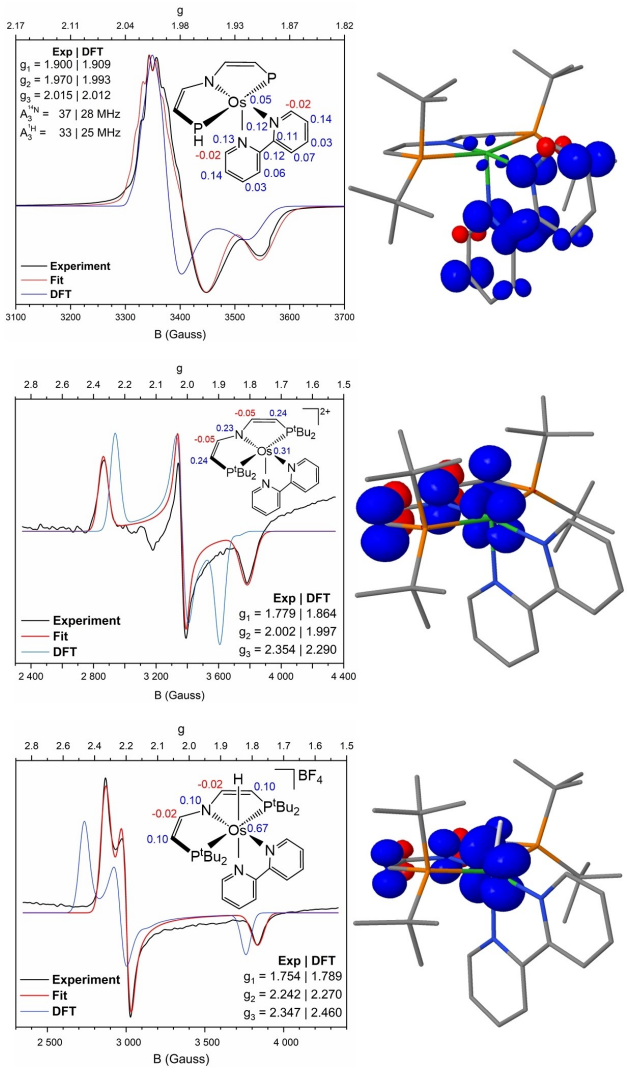

Figure 3. *Left*: Experimental (black), simulated (red), and DFT computed (blue) X-band EPR spectra of **4** (top, 140 K), $\mathbf{5}^{\mathbf{2BArF}}$ (centre, 140 K) and $\mathbf{7}^{\mathbf{BF4}}$ (bottom, 150 K) in THF; insets: selected α (blue) and β (red) Löwdin spin populations. *Right*: DFT computed spin density plots of **4** (top) $\mathbf{5}^{\mathbf{2BArF}}$ (centre), and $\mathbf{7}^{\mathbf{BF4}}$ (bottom).

(Figure 2) by a long bond in *trans*-position (d_{Os-N3} = 2.096(5) Å) with respect to parent **2** (d_{Os-N3} = 2.031(2) Å) or $\mathbf{3}^{\mathbf{BPh4}}$ (d_{Os-N3} = 2.039(3) Å).

The CV of **6** in THF revealed two reversible oxidation waves at E_1^0 =-0.96 V and E_2^0 = 0.06 V (v = 100 mV s^{-1}), respectively (Figure 2, right).[21] DFT excellently reproduced the first oxidation (E_1^{DFT} = −1.00 V) but failed for the second by a relatively large margin (E_2^{DFT} = 0.57 V). The $Os^{III/II}$ couple exhibits a remarkably low potential compared to other Os^{II} hydrides,[7] which is attributed to the strong σ/π-donating ability of the pincer ligand.[9a] Comparison of E_2^0 is hampered by the scarcity of $Os^{IV/III}$ hydrido reference data. Bianchini *et al.* reported that $[Os^{II}HCl(PP_3)]$ (PP_3 = $P(CH_2CH_2PPh_2)_3$) undergoes two closely spaced oxidations (E_1^0 = −0.23 V; $E_2^{p,a}$ = −0.08 V).[22] In that case, the irreversibility of the second oxidation was attributed to rapid deprotonation of $[Os^{IV}HCl(PP_3)]^{2+}$ within an EEC mechanism. For Taube's hydride $[Os^{III}(en)_2(py)H)]^{2+}$, an irreversible oxidation was reported at E = 0.95 V.[8]

UV-vis spectroelectrochemistry (Figure 4) gave isosbestic points for the first oxidation of **6** (E_{appl} = −0.9 V), but not for the second (E_{appl} = 0.1 V), indicating rapid decay of the primary 2-electron oxidation product. *In situ* spectroscopic examination after the oxidation of **6** with 2 eq. of $AgBAr^F_4$ at low temperatures (< −70 °C) showed the formation of NMR silent products. With X-band EPR, several signals with large g anisotropy were observed. Notably, the formal deprotonation product, diamagnetic $\mathbf{3}^+$, was not found in the NMR spectrum, and EPR indicated a more complex decomposition pathway to multiple osmium(III) species. Unfortunately, unequivocal assignment of all EPR signals was not possible. To this end, the fate of the product from 2-electron oxidation remains unknown and we subsequently focused on the synthesis of the 1-electron oxidation product.

Chemical oxidation of **6** with 1 eq. of $AgBF_4$ or $[Fe(Cp^*)_2]BF_4$ in THF provided the osmium(III) hydride $[Os^{III}H(PNP)(bipy)]BF_4$ ($\mathbf{7}^{\mathbf{BF4}}$) in 42% isolated yield (Scheme 1). Paramagnetic $\mathbf{7}^+$ exhibits a very broad ^{1}H NMR signal. Preservation of the Os–H bond is confirmed by an IR band at $\tilde{\nu}_{Os-H}$ = 2115 cm^{-1} (DFT: 2141 cm^{-1}), which is even higher than that of Taube's $[Os^{III}H(en)_2(py)](OTf)_2$ ($\tilde{\nu}$ = 2020 cm^{-1}).[8] The oxidation-induced increase by 15 cm^{-1} is within the range that was found empirically by Morris as an effect of the additional positive charge ($\triangle\tilde{\nu} = 25 \pm 10$ cm^{-1}).[23] Structural characterization of $\mathbf{7}^{\mathbf{BF4}}$ by single-crystal X-ray diffraction (Figure 2) confirmed the presence of the tetrafluoroborate anion. The hydride ligand could be found in the difference electron density map. The relatively long bond in *trans*-position (d_{Os-N3} = 2.141(3) Å) further supports the presence of the hydrido ligand.

X-band EPR spectroscopy of $\mathbf{7}^+$ (Figure 3) confirmed a doublet ground state with similar g-anisotropy, yet significantly lower rhombicity (g = 2.35, 2.24, 1.75) with respect to five-coordinate $\mathbf{5}^{2+}$, allowing for safe discrimination. DFT computations (g_{DFT} = 2.46, 2.27, 1.79) reproduced the EPR spectrum sufficiently well. As in case of $\mathbf{5}^{2+}$, the SOMO exhibits predominant $\pi^*(d_{yz}/p_z)$ character, yet with decreased ligand redox non-innocence, i.e., 30% ($\mathbf{7}^+$) vs. 70% ($\mathbf{5}^{2+}$) localization of the majority spin carrier density at the pincer ligand. This can

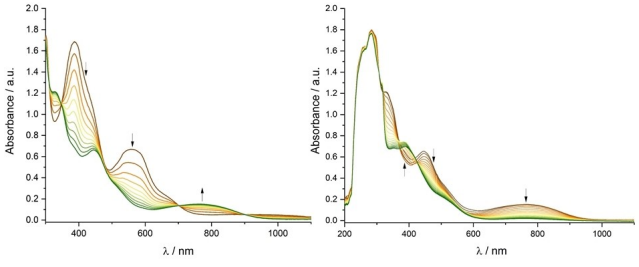

Figure 4. UV − vis spectroelectrochemistry (SEC) for the oxidation of **6** in THF (2 mM, 0.2 M $[nBu_4N][PF_6]$, 25 °C) at E_{appl} = −0.9 V (left) and E_{appl} = 0.1 V (right), respectively, over 6 min with spectra recorded every 12 sec.

be attributed to slightly reduced π-bonding as a result of the additional hydrido donor. Nevertheless, increased Os–N_{PNP} π-interaction with respect to parent **6** is reflected by significant shortening of the Os–N1 bond ($d = 2.012(4)$ Å (**7**$^+$) vs. 2.103(5) Å (**6**)). Thus, the relatively low potential of the **7**$^+$/**6** redox couple can be partially attributed to the π-donating nature of the divinylamido ligand.

PCET thermochemistry of the osmium hydrides. Notably, **7**$^+$ is only the second isolable Os^{III} hydride reported in the literature. To further analyze its remarkable stability, the thermochemistry for Os–H proton-coupled electron transfer (PCET) was examined (Scheme 2). The square scheme was anchored with the electrochemical data of **3**$^+$ and **6**, as well as the computed $BDFE_{Os–H}$ of the **7**$^+$/**3**$^+$ PCET couple, due to good agreement of computed structural and spectroscopic data for these compounds with experiment. All other values were calculated via Bordwell's equation, using Mayer's standard potential for the H^+/H couple in THF *vs.* Fc^+/Fc (C_G = 59.9 kcal mol^{-1}):[24]

$$BDFE = 23.06 \bullet E^0 + 1.37 \bullet pK_a + C_G$$

The high $BDFE_{Os–H}$ of osmium(II) complex **6** (72 kcal mol^{-1}; $BDFE_{Os–H}^{DFT}$ = 70 kcal mol^{-1}) is in the typical range of previous reports in the literature (58-78 kcal mol^{-1}), such as Bianchini's osmium(II) complex [$Os^{II}HCl(PP_3)$] ($BDFE_{Os–H}^{THF}$ = 68 kcal mol^{-1}).[7,22,25] Oxidation of **6** comes with a reduction of the $BDFE_{Os–H}$ to 52 kcal mol^{-1}, which is, in fact, identical with the reported $BDFE_{Os–H}$ for [$Os^{III}HCl(PP_3)$]$^+$. Thus, as previously stated by Morris and co-workers,[7] the Os–H bond strength is not dramatically lowered by oxidation, but △BDFE seems remarkably robust. Notably, in our case the presence of redox non-innocent ligands, i.e., on one hand the PNP ligand in the hydrido radical cation (**7**$^+$) and on the other hand the bipy ligand in five-coordinate **4**, does not have a major effect on $BDFE_{Os–H}$. Emslie and Morris recently reported for a series of manganese hydrido complexes that the ligand *trans* to the hydride (PMe_3, C_2H_4, CO) had a significant impact on the relative $BDFE_{Mn–H}$ of Mn^I vs. Mn^{II} hydrides.[26] In the current case, the bipy ligand might qualitatively be considered as intermediate with respect to this manganese series. While further variation of the ligand framework is required for full rationalization, our observations apparently indicate pK_a/potential compensation between the acidic (Os–H) and the redox active sites.

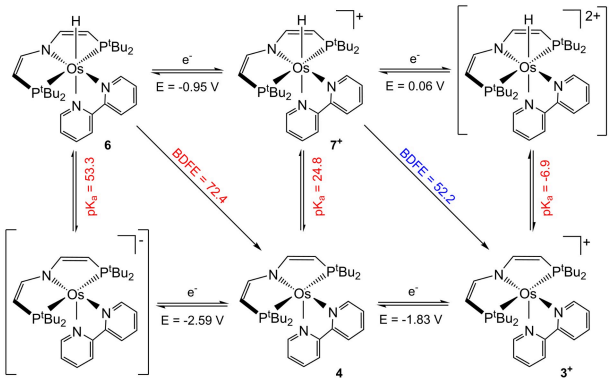

Scheme 2. Thermochemical square scheme for Os–H PCET (BDFEs in kcal mol^{-1}). Species that were not spectroscopically characterized are shown in square brackets. The DFT computed value is provided in blue, experimental data in black, and red data was calculated via Bordwell's equation.

The bond strength of the Os^{III}–H bond actually is close to half the BDFE of H_2, suggesting intrinsic instability towards hydrogen evolution. However, control experiments showed that **7**$^+$ does not react with an excess of PCET reagents like 2,4,6-tri-tert-butylphenoxy radical ($BDFE^{THF}$(H–$OC_6tBu_3H_2$) = 74.4 kcal mol^{-1}) or 2,2,6,6-tetramethylpiperidin-1-yl)oxyl radical ($BDFE^{THF}$(TEMPO–H) = 65.5 kcal mol^{-1}).[6] Thus, the chemical stability of **7**$^+$ with respect to H-atom transfer is also attributed to kinetic reasons, presumably due to steric shielding of the hydride ligand by the pincer *tert*-butyl groups.

The acidity of **7**$^+$ (pK_a = 25) is almost 30 pK_a units lower than the estimate for **6**, (Scheme 2), which is in the typical range for oxidation-induced pK_a reduction of hydrido complexes.[7] Further reduction of the pK_a by a similar magnitude was estimated for the second oxidation. Note that this potential was not well reproduced by DFT and might rather be a lower limit, in turn rendering the pK_a as upper limit. Albeit the fate of [OsH(PNP)(bipy)]$^{2+}$ could ultimately not be clarified, it is tempting to speculate that its decay is associated with proton loss. Nevertheless, the chemical stability of the hydrido radical cation **7**$^+$ can also be attributed to its high pK_a and the sizable difference of its reduction and oxidation potentials ($\triangle E^0$ = 1.0 V), which prevents decay via [OsH(PNP)(bipy)]$^{2+}$ due to disproportionation ($K_{disp} \approx 10^{-17}$).

Conclusion

In summary, we reported the synthesis of **7**$^+$ as the second isolable osmium(III) hydrido complex and attributed the stability to several features. Thermochemical characterization revealed the significant reduction of the $BDFE_{Os–H}$ with respect to parent **6**, close to the bond strength of dihydrogen. Steric shielding might therefore be a contributing factor to prevent H_2 evolution. Notably, the redox non-innocence of the ligands in the PCET donor state **7**$^+$ and acceptor state **4** does not seem to have a major effect on the absolute and the relative BDFEs of the hydrides **6** and **7**$^+$.

The estimated drops of the pK_a upon 1- and 2-electron oxidation of **6**, respectively, are in the typical ranges of related hydrides. Thus, the high pK_a of parent **6** is an important prerequisite for the stability of **7**$^+$ with respect to proton loss, emphasizing the importance of strongly donating ligands. The well separated oxidation and reduction potentials of **7**$^+$ prevent decomposition via disproportionation to the unstable dication. This is a direct consequence of the rather low $Os^{III/II}$ potential, which can in part be associated with the stabilization of the radical **7**$^+$ by ligand non-innocence. Thus, ligand redox activity ultimately seems to have an indirect impact on its chemical stability.

Experimental Section

Materials and Methods. All experiments were carried out under Argon using Schlenk and glovebox techniques. All solvents were purchased in HPLC quality (Sigma Aldrich/Merck), and dried using an MBRAUN Solvent Purification System. Deuterated solvents were obtained from Euriso-Top GmbH, dried over Na/K (THF, Benzene), distilled by trap-to-trap transfer *in vacuo*, and degassed by three freeze–pump–thaw cycles, respectively. $Fe(Cp)_2$ was sublimed at 40 °C/0.020 mbar. [*n*-Bu_4N]PF_6 from Sigma Aldrich was dried at 80 °C/0.005 mbar before use. The starting complex **1**,[12] $AgBAr^F{}_4$[27] and 2,4,6-tri-tert-butylphenoxy radical (TBP)[28] radical were prepared according to literature procedures. $NaBAr^F$ was purchased from Sigma Aldrich, recrystallized in Et_2O and dried under vacuum at 30 °C/0.5·10^{-4} mbar, respectively. All other commercially available chemicals were used without further purification.

Cyclic voltammograms were recorded with a Metrohm Autolab PGSTAT101 using an Ag/Ag^+ reference, a glassy-carbon working and a Pt-wire counter electrode. Experimental X-band EPR spectra were recorded on a Bruker ELEXSYS-II E500 CW-EPR. The spectra were simulated using the EPR-simulation program EasySpin.[29] IR spectra were obtained as powder on a Bruker ALPHA FT-IR spectrometer with Platinum ATR module at room temperature. Elemental analyses were obtained from the analytical laboratories at the Georg-August University on an Elementar Vario EL 3. NMR Spectra were recorded on Bruker Avance III 300, Bruker Avance III 300 and Bruker Avance III 400 and were calibrated to the residual solvent proton resonance. (d_6-Benzene: $\delta_H = 7.16$ ppm, d_8-THF: $\delta_H = 1.73, 3.58$ ppm). Due to a lack of resolution in 2D NMR experiments, we refrained from an assignment of the bipyridine signals in NMR. LIFDI spectrometry was performed on a Joel AccuTOF spectrometer under inert conditions.

Crystallographic Details. Suitable single crystals for X-ray structure determination were selected from the mother liquor under an inert gas atmosphere and transferred in protective perfluoro polyether oil on a microscope slide. The selected and mounted crystals were transferred to the cold gas stream on the diffractometer. The diffraction data were obtained at 100 K on a Bruker D8 three-circle diffractometer, equipped with a PHOTON 100 CMOS detector and an INCOATEC microfocus source with Quazar mirror optics (Mo-K_α radiation, $\lambda = 0.71073$ Å). The data obtained were integrated with SAINT and a semi-empirical absorption correction from equivalents with SADABS was applied. The structure was solved and refined using the Bruker SHELX 2014 software package.[30] All non-hydrogen atoms were refined with anisotropic displacement parameters. All C–H hydrogen atoms were refined isotropically on calculated positions by using a riding model with their U_{iso} values constrained to 1.5 U_{eq} of their pivot atoms for terminal sp^3 carbon atoms and 1.2 times for all other atoms.

DFT Computations. Structure and energy calculations were performed within the ORCA 4.1.1 program suite.[31] Molecular structures were optimized using the PBE functional,[32] Grimme's dispersion correction with Becke-Johnson damping (D3(BJ))[33] and the Resolution of Identity approach (RI-*J*)[34] to minimize computational costs. Ahlrichs' revised def2-SVP basis set and the corresponding auxiliary basis set were used with an all-electron basis for all elements but Os for which a Stuttgart-Dresden 60 electron core potential replaced the inner shell 1s–4f orbitals.[35] Tight convergence criteria in the SCF procedure and structure optimization and a fine integration grid (Grid5) were applied and the optimized (gas phase) structures were defined as minima by analytical vibrational analyses. The electronic energies were evaluated by single point calculations applying the M06[36] functional, Ahlrichs' def2-TZVP basis set and Truhlar's SMD solvation model (THF).[37] Finally, thermodynamic data were computed by applying Grimme's quasi-RRHO approach.[38] All free energies were further corrected for standard solution conditions (1 mol L^{-1}, 298.15 K) by adding 1.89 kcal mol^{-1}. The free energy correction of H• was obtained from the translational and electronic partition function and corrected for standard solution conditions:

$$G(H\bullet) = -RT(lnq_{trans} + lng_0) + 1.89\ \text{kcal}\cdot\text{mol}^{-1} = -4.78\ \text{kcal}\cdot\text{mol}^{-1}.$$

Redox potentials were evaluated as previously described.[39] EPR data were obtained[40] with the ADF program[41] employing the two-component ZORA formalism implemented in ADF,[42] the PBE0 hybrid functional[43] and the TZP Slater type orbital basis set.[44]

Synthesis of 2. [$OsCl_2${$N(CHCHP^tBu_2)_2$}] (**1**, 5.0 mg, 8.1 μmol, 1.0 eq.) and $CoCp_2$ (1.5 mg, 8.1 μmol, 1.0 eq.) are dissolved in benzene (2 mL) and stirred for 2 min at RT and filtered. 2,2′-bipyridine (1.3 mg, 8.1 μmol, 1.0 eq) in benzene (2 mL) is added and stirring is continued for 5 min. The solvent is evaporated, and the crude product is washed with pentane (2x 2 mL) and extracted with benzene (3x 1 mL). Lyophilization yields **2** (4.4 mg, 6.0 μmol, 74%) as a red powder. Anal. Calcd. for $C_{30}H_{48}ClN_3OsP_2$ (738.36): C, 48.80; H, 6.55; N, 5.69 Found: C, 49.2; H, 7.00; N, 5.40. ^{1}H NMR (THF-d_8, RT, 400 MHz): δ = 11.04 (d, $^3J_{HH}$ = 6.1 Hz, 1 H, bipy), 8.29 (d, $^3J_{HH}$ = 6.1 Hz, 1 H, bipy), 8.18 (dd, $^3J_{HH}$ = 8.2 Hz, $^4J_{HH}$ = 1.6 Hz, 1 H, bipy), 8.00 (dd, $^3J_{HH}$ = 8.1 Hz, $^4J_{HH}$ = 1.8 Hz, 1 H, bipy), 7.55 ($A_9BCXX'A'_9B'C'$, $N = |{}^3J_{CX} + {}^4J_{CX'}| = 33.4$ Hz, $^3J_{BC}$ = 5.9 Hz, 2 H, NC*H*CHP), 7.35 (m, 1 H, bipy), 7.20 (dd, $^3J_{HH}$ = 13.3 Hz, $^4J_{HH}$ = 1.6 Hz, 1 H, bipy), 7.02 (m, 1 H, bipy), 6.73 (ddd, $^3J_{HH}$ = 13.3 Hz, 6.6 Hz, $^4J_{HH}$ = 1.6 Hz, 1 H, bipy), 3.96 ($A_9BCXX'A'_9B'C'$, $N = |{}^2J_{BX} + {}^4J_{BX'}| = 4.1$ Hz, $^3J_{BC}$ = 6.0 Hz, 2 H, NCHC*H*P), 1.65 ($A_9BCXX'A'_9B'C'$, $^3J_{AX}$ = 8.5 Hz, 18 H, P(C(CH_3)$_3$)), 0.32 ($A_9BCXX'A'_9B'C'$, $^3J_{AX}$ = 8.3 Hz, 18 H, P(C(CH_3)$_3$)). ^{13}C{^{1}H}-NMR (THF-d_8, RT, 101.25 MHz): δ = 165.1 (s, bipy), 153 (vt, $^2J_{CP}$ = 7.5 Hz, NCHCHP), 137.0 (s, bipy), 153.1 (s, bipy), 130.2 (s, bipy), 128.0 (s, bipy), 127.0 (s, bipy), 125.4 (s, bipy), 127.7 (s, bipy), 123.9 (s, bipy), 85.2 (vt, $^1J_{CP}$ = 18.7 Hz, NCH*C*HP), 30.0 (vt, $^1J_{CP}$ = 10.5 Hz, P(*C*(CH_3)$_3$)$_2$), 29.1 (vt, $^1J_{CP}$ = 8.5 Hz, P(*C*(CH_3)$_3$)$_2$), 25.8 (s br, P(C(*C*H_3)$_3$)$_2$). ^{31}P{1H}-NMR (THF-d_8, RT, 161.25 MHz): δ = 19.2. MS (LIFDI, toluene) m/z = 739.1 ([M^+]), 704.2 ([M–Cl^+]).

Synthesis of 3^{BPh4}. Complex **1** (100 mg, 0.16 mmol, 1.0 eq) and $CoCp_2$ (30.25 mg, 0.16 mmol, 1.0 eq) are dissolved in benzene and stirred for 1 min after which 2,2′-bipyridine (24.9 mg, 0.16 mmol, 1.0 eq) was added to the mixture. After 30 min, the reaction mixture was filtered and the residue on the filter was washed with pentane. The solvent was removed under vacuum and the crude product (78.3 mg, 0.11 mmol, 1.0 eq, 66%) was dissolved in THF. $NaBPh_4$ (37.6 mg, 0.11 mmol, 1.0 eq) was added to the solution and the mixture was stirred for 5 min. The reaction mixture was filtered, and the residue was extracted with THF. The solvent amount was reduced and then layered with pentane. After crystallization at −35 °C for at least 16 h, the solid was washed with pentane and the product was extracted with dichloromethane. The solvent was removed and $\mathbf{3}^{BPh4}$ was formed as orange-brown solid (81.2 mg, 0.08 mmol, 48%). Anal. Calcd. for $C_{54}H_{68}BN_3OsP_2$ (1023.46): C, 63.45; H, 6.71; N, 4.11; Found: C, 63.8; H, 6.53; N, 3.81. ^{1}H-NMR: (d_8-THF, RT, 300 MHz): δ = 9.09 (s br, 2H, bipy), 7.95 (d, $^3J_{HH}$ = 8.1 Hz, 2 H, bipy), 7.81 ($A_{18}BXX'A'_{18}B'C'$, $N = |{}^3Jcx + 4Jcx'| = 35.4$ Hz, $^3J_{BC}$ = 5.8 Hz, 2 H, NC*H*CHP), 7.49 (t, $^3J_{HH}$ = 7.9 Hz, 2 H, bipy), 7.34 (t, $^3J_{HH}$ = 6.1 Hz, 8 H, BPh_4: *o*-H), 7.16 (t, $^3J_{HH}$ = 7.0 Hz, 2H, bipy), 6.85 (t, $^3J_{HH}$ = 7.3 Hz, 8 H, BPh_4: *m*-H), 6.68 (t, $^3J_{HH}$ = 7.1 Hz, 4 H, BPh_4: *p*-H), 4.37 ($A_{18}BXX'A'_{18}B'C'$, $N = |{}^2J_{BX} + {}^4J_{BX}| = 5.9$ Hz, $^3J_{BC}$ = 5.8 Hz, 2 H, NCHC*H*P), 0.49 ($A_{18}XX'A'_{18}$, $N = |{}^3J_{AX} + {}^5J_{AX'}| = 13.1$ Hz, 36 H, P(C(CH_3)$_3$)$_2$). ^{13}C{^{1}H}-NMR (101.25 MHz): δ = 165.6 (vt, $^2J_{CP}$ = 7.5 Hz, NCHCHP), 165.4 (q, $^1J_{C}{}^{11}{}_{B}$ = 49 Hz, BPh_4: C_i), 163.1 (s, bipy), 157.6 (s, bipy), 137.4 (q, $^1J_{CB}$ = 1.6 Hz, BPh_4: C_o), 135.7 (s, bipy), 127.7 (s, bipy), 126.0 (q, $^1J_{CB}$ = 2.7 Hz, BPh_4: C_m), 125.3 (s, bipy), 122.1 (s, BPh_4: C_p),

86.1 (vt, $^{1}J_{CP}$ = 21.5 Hz, NCHCHP), 66.4 (s br, P(*C*(CH$_3$)$_3$)$_2$), 28.1 (s, P(C(CH$_3$)$_3$)$_2$). ^{31}P{^{1}H}-NMR (161.25 MHz): δ = 26.7 (s, P(C(CH$_3$)$_3$)$_2$)).

Synthesis of 3^{BArF}. Complex **1** (100 mg, 0.16 mmol, 1.0 eq) and $CoCp_2$ (30.25 mg, 0.16 mmol, 1.0 eq) are dissolved in benzene and stirred for 1 min after which 2,2′-bipyridine (24.9 mg, 0.16 mmol, 1.0 eq) was added to the mixture. After 30 min, the reaction mixture was filtered and the residue on the filter was washed with pentane. The solvent was removed under vacuum and the crude product (71.4 mg, 0.10 mmol, 1.0 eq, 60%) was dissolved in diethyl ether. $NaBAr^F_4$ (88.8 mg, 0.10 mmol, 1.0 eq) was added to the solution and the mixture was stirred for 5 min. The reaction mixture was filtered, and the residue was extracted with diethyl ether. The solvent amount was reduced and then layered with pentane. After crystallization at −35 °C for at least 16 h, the solid was washed with pentane and the product was extracted with dichloromethane. The solvent was removed and **3^{BArF}** was formed as orange-brown solid (78.4 mg, 0.05 mmol, 31%). Anal. Calcd. for $C_{62}H_{60}BF_{24}N_3OsP_2$ (1566.13): C, 47.55; H, 3.86; N, 2.68; Found: C, 47.72; H, 3.93; N, 2.06. ^{1}H-NMR (d$_8$-THF, RT, 400 MHz): δ = 9.23 (s br, 2 H, bipy), 8.4 (d, $^{3}J_{HH}$ = 8.1 Hz, 2 H, bipy), 7.9–7.8 (A_{18}BXX′A′$_{18}$B′C′, partially covered, $^{3}J_{BC}$ = 5.8 Hz, 2 H, NC*H*CHP), 7.79 (t, $^{3}J_{HH}$ = 2.5 Hz, 8 H, BAr^F_4: *o*-H), 7.74 (t, $^{3}J_{HH}$ = 7.9 Hz, bipy), 7.58 (br s, 4 H, BAr^F_4, *p*-H), 7.38–7.29 (m, 2 H, bipy), 4.4 (A_{18}BXX′A′$_{18}$B′C′, $N = |^{2}J_{BX} + {}^{4}J_{BX}| = 5.7$ Hz, $^{3}J_{BC}$ = 5.8 Hz, 2 H, NCHC*H*P), 0.52 (A_{18}XX′A′$_{18}$, $N = |^{3}J_{AX} + {}^{5}J_{AX'}| = 13.1$ Hz, 36 H, P(C-(CH$_3$)$_3$)$_2$). ^{13}C{^{1}H}-NMR (101.25 MHz): δ = 165.7 (t, $^{2}J_{CP}$ = 7.8 Hz, NCHCHP), 163.0 (q, $^{1}J_{C11B}$ = 49.5 Hz, 4 C, BAr^F_4: C_i), 135.8 (br s, BAr^F_4: C_o), 135.4 (s, C_c), 130.3 (qq, $^{2}J_{CF}$ = 31.6 Hz, $^{3}J_{CB}$ = 3.2 Hz, BAr^F_4: C_m), 127.9 (br s, bipy), 125.7 (q, $^{1}J_{CF}$ = 274 Hz, BAr^F_4: CF_3), 124.9 (s, bipy), 118.4 (hept, $^{3}J_{CF}$ = 4.0 Hz, BAr^F_4: C_p), 86.1 (t, $^{1}J_{CP}$ = 21.0 Hz, NCHCHP), 43.3 (s, P(*C*(CH$_3$)$_3$)$_2$), 26.9 (s, P(C(*C*H$_3$)$_3$)$_2$). ^{31}P{^{1}H}-NMR (161.25 MHz): δ = 26.9 (s, P(C(CH$_3$)$_3$)$_2$)).

Spectroscopic characterization of 4. Complex **3^{BPh4}** (5.0 mg, 4.9 µmol, 1.0 eq) and Na/Hg (2 M, 0.33 g, 49 µmol, 10 eq) were suspended in 1 mL of THF and stirred for 1 minute at RT. The solution was filtered and immediately frozen with liquid N_2 and transferred to the EPR spectrometer for characterization.

Synthesis of 5^{2BArF}. Complex **3^{BArF}** (20.0 mg, 12.8 µmol, 1.0 eq) and $AgBAr^F_4$ (12.4 mg, 12.8 µmol, 1.0 eq) were dissolved in 5 mL of THF at −80 °C. The solution was stirred for 5 min at −80 °C and filtered, keeping the mixture at the same temperature. After this, the solution was cooled down for EPR spectroscopy. After measurement, the solvent was removed giving the product as dark brown solid (16.3 mg, 6.7 µmol, 53%). Anal. Calcd. for $C_{94}H_{72}B_2F_{48}N_3OsP_2$ (2429.36): C, 46.47; H, 2.99; N, 1.73. Found: C, 46.9; H, 2.78; N, 1.81.

Synthesis of 6. Complex **3^{BPh4}** (70.0 mg, 0.07 mmol, 1.0 eq) was dissolved in THF. $NaBH_4$ (51.8 mg, 1.36 mmol, 20.0 eq) was added to the solution and the mixture was stirred for at least 6 hours for the product to be formed. The solvent was removed, and the product was extracted using pentane. Lyophilization yields **6** as dark green powder (28 mg, 0.04 mmol, 58%). Anal. Calcd. for $C_{30}H_{49}N_3OsP_2$ (703.92): C, 51.2; H, 7.02; N, 5.97. Found: C, 51.4; H, 7.10; N, 5.90. ^{1}H-NMR (C_6D_6, RT, 400 MHz): δ = 10.26 (d, $^{3}J_{HH}$ = 6.2 Hz, 1H, bipy), 8.69 (d, $^{3}J_{HH}$ = 5.9 Hz, 1H, bipy), 7.52 (A_9BXX′A′$_9$B′C′, $N = |^{3}J_{CX} + {}^{4}J_{CX'}| = 34.0$ Hz, $^{3}J_{BC}$ = 5.5 Hz, 2 H, NC*H*CHP), 7.36 (br s, 1 H, bipy), 7.33 (br s, 1 H, bipy), 6.73–6.68 (m, 1 H, bipy), 6.65-6.61 (m, 1 H, bipy), 6.37–6.33 (m, 1 H, bipy), 6.09–6.04 (m, 1 H, bipy), 4.26 (A_9BXX′A′$_9$′C′, $N = |^{2}J_{BX} + {}^{4}J_{BX'}| = 5.5$ Hz, $^{3}J_{BC}$ = 5.5 Hz, 2 H, NCHC*H*P), 1.57 (A_9BCXX′A′$_9$B′C′, $^{3}J_{AX}$ = 12.5 Hz, 18 H, P(C(CH$_3$)$_3$)), 0.45 (A_9BCXX′A′$_9$B′C′, $^{3}J_{AX}$ = 12.2 Hz, 18 H, P(C(CH$_3$)$_3$)), −11.0 (t, $^{3}J_{HP}$ = 24.2 Hz, Os–H). ^{13}C{^{1}H}-NMR (C_6D_6, RT 101.25 MHz): δ = 162.0 (vt, $^{2}J_{CP}$ = 9.0 Hz, NCHCHP), 160.8 (s, bipy), 160.6 (s, bipy), 159.8 (s, bipy), 149.8 (s, bipy), 125.7 (s, bipy), 126.1 (s, bipy), 125.4 (s, bipy), 124.9 (s, bipy), 124.2 (s, bipy), 123.2 (s, bipy), 85.7 (vt, $^{1}J_{CP}$ = 19.2 Hz, NCHCHP), 41.3 (vt, $^{1}J_{CP}$ = 8.5 Hz, P(*C*(CH$_3$)$_3$)$_2$), 40.0 (vt, $^{1}J_{CP}$ = 13.9 Hz, P(*C*(CH$_3$)$_3$)$_2$), 30.5 (s br, P(C(CH$_3$)$_3$)$_2$), 29.9 (vt, $^{2}J_{CP}$ = 2.5 Hz, P(C(CH$_3$)$_3$)$_2$). ^{31}P{^{1}H}-NMR (C_6D_6, RT, 161.25 MHz): δ = 51.5 (s, P(C(CH$_3$)$_3$)$_2$)). IR (ATR, RT) ν = 2100 cm^{-1} (Os–H).

Synthesis of 7^{BF4}. Complex **6** (15.0 mg, 21.2 µmol, 1.0 eq) was dissolved in THF. $[Fe(Cp^*)_2]BF_4$ (8.7 mg, 21.2 µmol, 1.0 eq) was added to the solution and the mixture was stirred for 10 min. The reaction mixture was filtered, followed by solvent evaporation. The crude product is washed with ether (4x 3 mL) and the paramagnetic compound, **7^{BF4}** is formed as orange-brown solid (7.8 mg, 9.3 µmol, 42%). Anal. Calcd. for $C_{30}H_{49}BF_4N_3OsP_2$ (790.72): C, 45.57; H, 6.25; N, 5.31. Found C, 45.2; H, 6.8; N, 5.4. IR (ATR, RT) ν = 2115 cm^{-1} (Os–H).

Supporting Information

NMR spectra, crystallographic data and DFT results are provided in the supporting information.

Acknowledgements

This work was funded by the Deutsche Forschungsgemeinschaft through SFB 1073 *Atomic Scale Control of Energy Conversion* (project C07) and the Fonds der Chemischen Industrie (FCI Doktoranden Stipendium for J.A.). The authors thank Dr. Christian Volkmann for crystallographic characterization of **3^{BPh4}**. Open Access funding enabled and organized by Projekt DEAL.

Conflict of Interest

The authors declare no conflict of interest.

Data Availability Statement

The data that support the findings of this study are available from the corresponding author upon reasonable request.

Keywords: Osmium · Hydrido Complexes · Proton-coupled Electron Transfer · Electrochemistry · Density Functional Theory

[1] a) F. Kallmeier, R. Kempe, *Angew. Chem. Int. Ed.* **2018**, *57*, 46; b) T. Irrgang, R. Kempe, *Chem. Rev.* **2019**, *119*, 2524.
[2] J. C. Babón, M. A. Esteruelas, A. M. López, *Chem. Soc. Rev.* **2022**, *51*, 9717.
[3] R. Poli, *Paramagnetic Mono- and Polyhydrides of the Transition Metals. In Recent Advances in Hydride Chemistry* (Eds.: M Peruzzini, R. Poli), Elsevier, Amsterdam, **2001**, pp. 139.
[4] Y. Hu, A. P. Shaw, D. P. Estes, J. R. Norton, *Chem. Rev.* **2016**, *116*, 8427.
[5] a) O. B. Ryan, M. Tilset, V. D. Parker, *J. Am. Chem. Soc.* **1990**, *112*, 2618; b) M. Tilset, *J. Am. Chem. Soc.* **1992**, *114*, 2740; c) V. Skagestad, M. Tilset, *J. Am. Chem. Soc.* **1993**, *115*, 5077.
[6] C. F. Wise, R. G. Agarwal, J. M. Mayer, *J. Am. Chem. Soc.* **2020**, *142*, 10681–10691.
[7] B. E. Rennie, R. G. Eleftheriades, R. H. Morris, *J. Am. Chem. Soc.* **2020**, *142*, 17607.

[8] J. S. McQueen, N. Nagao, T. Eberspacher, Z. W. Li, H. Taube, *Inorg. Chem.* **2003**, *42*, 3815.
[9] a) S. Schneider, J. Meiners, B. Askevold, *Eur. J. Inorg. Chem.* **2012**, 412; b) L. Alig, M. Fritz, S. Schneider, *Chem. Rev.* **2019**, *119*, 2681.
[10] F. Schneck, M. Finger, M. Tromp, S. Schneider, *Chem. Eur. J.* **2017**, *23*, 33.
[11] W. Kaim, *Inorg. Chem.* **2011**, *50*, 9752.
[12] a) J. Abbenseth, M. Diefenbach, S. C. Bete, C. Würtele, C. Volkmann, S. Demeshko, M. C. Holthausen, S. Schneider, *Chem. Commun.* **2017**, *53*, 5511; b) J. Abbenseth, S. C. Bete, C. Volkmann, C. Würtele, S. Schneider, *Organometallics* **2018**, *37*, 802; c) J. Ramler, K. Radacki, J. Abbenseth, C. Lichtenberg, *Dalton Trans.* **2020**, *49*, 9024.
[13] A. W. Addison, T. N. Rao, J. Reedijk, J van Rijn, G. C. Verschoor, *J. Chem. Soc., Dalton Trans.* **1984**, 1349.
[14] All redox potentials are reported *vs.* $FeCp_2^+/FeCp_2$.
[15] N. G. Connelly, W. E. Geiger, *Chem. Rev.* **1996**, *96*, 877.
[16] The spectrum can also be satisfactorily fitted using HFI with two ^{14}N and two ^{31}P nuclei. In fact, DFT showed similar HFI constants for ^{1}H and ^{31}P. We here provide the minimum model to avoid overfitting. Importantly, all satisfactory fits required HFI with two ^{14}N nuclei, thus supporting the bipy redox activity.
[17] W. Kaim, R. Reinhardt, M. Sieger, *Inorg. Chem.* **1994**, *33*, 4453.
[18] P. H. Rieger, *Coord. Chem. Rev.* **1994**, *135*, 203.
[19] R. H. Morris, *Inorg. Chem.* **2018**, *57*, 13809.
[20] a) J. Chatt, D. P. Melville, R. L. Richards, *J. Chem. Soc. A Inorganic, Phys. Theor.* **1971**, 895; b) J. V Caspar, B. P. Sullivan, T. J. Meyer, *Organometallics* **1983**, *2*, 551; c) B. P. Sullivan, J. V. Caspar, T. J. Meyer, S. Johnson, *Organometallics* **1984**, *3*, 1241; d) T. Wilczewski, *J. Organomet. Chem.* **1986**, *317*, 307; e) K. A. Earl, G. Jia, P. A. Maltby, R. H. Morris, *J. Am. Chem. Soc.* **1991**, *113*, 3027; f) C. Bianchini, K. Linn, D. Masi, M. Peruzzini, A. Polo, A. Vacca, F. Zanobini, *Inorg. Chem.* **1993**, *32*, 2366; g) M. T. Bautista, K. A. Earl, P. A. Maltby, R. H. Morris, C. T. Schweitzer, *Can. J. Chem.* **1994**, *72*, 547; h) T. Y. Bartucz, A. Golombek, A. J. Lough, P. A. Maltby, R. H. Morris, R. Ramachandran, M. Schlaf, *Inorg. Chem.* **1998**, *37*, 1555; i) W. S. Ng, G. Jia, M. Y. Hung, C. P. Lau, K. Y. Wong, L. Wen, *Organometallics* **1998**, *17*, 4556; j) T. A. Luther, D. M. Heinekey, *Inorg. Chem.* **1998**, *37*, 127.
[21] An additional, reversible reductive event at $E^0 = -2.66$ V is assigned to a bipy-centered reduction.
[22] C. Bianchini, M. Peruzzini, A. Ceccanti, F. Laschi, P. Zanello, *Inorg. Chim. Acta* **1997**, *259*, 61–70.
[23] R. H. Morris, *Inorg. Chem.* **2018**, *57*, 13809.
[24] R. G. Agarwal, S. C. Coste, B. D. Groff, A. M. Heuer, H. Noh, G. A. Parada, C. F. Wise, E. M. Nichols, J. J. Warren, J. M. Mayer, *Chem. Rev.* **2022**, *122*, 1.
[25] The BDFE data has been derived in a variety of different solvents. BDFEs usually show little solvent dependence (within 1–2 kcal mol^{-1}), as the charge and size of the acceptor and donor species do not change significantly (see ref. 6). However, more distinct variations can result from solvent coordination to the PCET acceptor state: F. Schneck, M. Finger, I. Siewert, S. Schneider, *Z. Anorg. Allg. Chem.* **2021**, *647*, 1478.
[26] B. E. Rennie, J. S. Price, D. J. H. Emslie, R. H. Morris, *Inorg. Chem.* **2023**, *62*, 8123.
[27] D. Coucouvanis, *Inorg. Synth.* **2002**, *33*, 86.
[28] V. W. Manner, T. F. Markle, J. H. Freudenthal, J. P. Roth, J. M. Mayer, *Chem. Commun.* **2008**, *246*, 256–258.
[29] S. Stoll, A. Schweiger, *J. Magn. Reson.* **2006**, *178*, 42–55.
[30] a) APEX3 v2016.9-0 (SAINT/SADABS/SHELXT/SHELXL), Bruker AXS Inc., Madison, WI, USA, **2016**; b) G. M. Sheldrick, *Acta Crystallogr. Sect. A* **2015**, *71*, 3; c) G. M. Sheldrick, *Acta Crystallogr. Sect. C* **2015**, *71*, 3; d) G. M. Sheldrick, *Acta Crystallogr. Sect. A* **2008**, *64*, 112.
[31] a) F. Neese, *Wiley Interdiscip. Rev.: Comput. Mol. Sci.* **2012**, *2*, 73; b) F. Neese, *Wiley Interdiscip. Rev.: Comput. Mol. Sci.* **2018**, *8*, 1327.
[32] J. P. Perdew, K. Burke, M. Ernzerhof, *Phys. Rev. Lett.* **1996**, *77*, 3865.
[33] a) S. Grimme, J. Antony, S. Ehrlich, H. Krieg, *J. Chem. Phys.* **2010**, *132*, 154104; b) S. Grimme, S. Ehrlich, L. Goerigk, *J. Comput. Chem.* **2011**, *32*, 1456.
[34] O. Treutler, R. Ahlrichs, *J. Chem. Phys.* **1995**, *102*, 346.
[35] a) D. Andrae, U. Häußermann, M. Dolg, H. Stoll, H. Preuß, *Theor. Chim. Acta* **1990**, *77*, 123; b) K. Eichkorn, O. Treutler, H. Öhm, M. Häser, R. Ahlrichs, *Chem. Phys. Lett.* **1995**, *242*, 652; c) K. Eichkorn, F. Weigend, O. Treutler, R. Ahlrichs, *Theor. Chim. Acc.* **1997**, *97*, 119; d) F. Weigend, M. Häser, H. Patzelt, R. Ahlrichs, *Chem. Phys. Lett.* **1998**, *294*, 143; e) F. Weigend, R. Ahlrichs, *Phys. Chem. Chem. Phys.* **2005**, *7*, 3297.
[36] Y. Zhao, D. G. Truhlar, *Theor. Chem. Acc.* **2007**, *120*, 215.
[37] A. V. Marenich, C. J. Cramer, D. G. Truhlar, *J. Phys. Chem. B* **2009**, *113*, 6378.
[38] S. Grimme, *Chem. Eur. J.* **2012**, *18*, 9955.
[39] B. Schluschaß, J. Abbenseth, S. Demeshko, M. Finger, A. Franke, C. Herwig, C. Würtele, I. Ivanovic-Burmazovic, C. Limberg, J. Telser, S. Schneider, *Chem. Sci.* **2019**, *10*, 10275.
[40] a) E. van Lenthe, P. E. S. Wormer, A. van der Avoird, *J. Chem. Phys.* **1997**, *107*, 2488; b) E. van Lenthe, A. van der Avoird, P. E. S. Wormer, *J. Chem. Phys.* **1998**, *108*, 4783.
[41] G. te Velde, F. M. Bickelhaupt, E. J. Baerends, C. F. Guerra, S. J. A. van Gisbergen, J. G. Snijders, T. Ziegler, *J. Comput. Chem.* **2001**, *22*, 931.
[42] a) E. van Lenthe, E. J. Baerends, J. G. Snijders, *J. Chem. Phys.* **1993**, *99*, 4597; b) E. van Lenthe, E. J. Baerends, J. G. Snijders, *J. Chem. Phys.* **1994**, *101*, 9783; c) E. van Lenthe, R. van Leeuwen, E. J. Baerends, J. G. Snijders, *Int. J. Quantum Chem.* **1996**, *57*, 281; d) E. van Lenthe, A. Ehlers, E.-J. Baerends, *J. Chem. Phys.* **1999**, *110*, 8943.
[43] C. Adamo, V. Barone, *J. Chem. Phys.* **1999**, *110*, 6158.
[44] E. van Lenthe, E. J. Baerends, *J. Comput. Chem.* **2003**, *24*, 1142.

Manuscript received: December 15, 2023
Revised manuscript received: January 22, 2024
Accepted manuscript online: January 23, 2024

